Shell model analysis of the neutrinoless double-β decay of ^{48}Ca

Mihai Horoi[1,*] and Sabin Stoica[2]

[1]*Department of Physics, Central Michigan University, Mount Pleasant, Michigan 48859, USA*

[2]*Horia Hulubei National Institute for Physics and Nuclear Engineering (IFIN-HH), 407 Atomistilor, Magurele-Bucharest, R-077125, Romania*

(Received 19 November 2009; published 23 February 2010)

The neutrinoless double-β ($0\nu\beta\beta$) decay process could provide crucial information to determine the absolute scale of neutrino masses, and it is the only one that can establish whether a neutrino is a Dirac or a Majorana particle. A key ingredient for extracting the absolute neutrino masses from $0\nu\beta\beta$ decay experiments is a precise knowledge of the nuclear matrix elements (NMEs) describing the half-life of this process. We developed a shell model approach for computing the $0\nu\beta\beta$ decay NME, and we used it to analyze the $0\nu\beta\beta$ mode of ^{48}Ca. The dependence of the NME on the short-range correlation parameters, on the average energy of the intermediate states, on the finite-size cutoff parameters, and on the effective interaction used for many-body calculations is discussed.

DOI: 10.1103/PhysRevC.81.024321 PACS number(s): 23.40.Bw, 21.60.Cs, 14.60.Pq, 27.40.+z

I. INTRODUCTION

Neutrinoless double-β ($0\nu\beta\beta$) decay, which can only occur by violating the conservation of the total lepton number, if observed, will unravel physics beyond the Standard Model (SM) and will represent a major milestone in the study of the fundamental properties of neutrinos [1–6]. Recent results from neutrino oscillation experiments have convincingly demonstrated that neutrinos have mass and they can mix [7–9]. Neutrinoless double-β decay is the most sensitive process to determine the absolute scale of the neutrino masses, and the only one that can distinguish whether a neutrino is a Dirac or a Majorana particle. A key ingredient for extracting the absolute neutrino masses from $0\nu\beta\beta$ decay experiments is a precise knowledge of the nuclear matrix elements (NMEs) for this process. Because most of the $\beta\beta$ decay emitters are open-shell nuclei, many calculations of the NMEs have been performed within the pnQRPA approach and its extensions [10–21]. However, the pnQRPA calculations are very sensitive to variation of the so-called g_{pp} parameter (the strength of the particle-particle interactions in the 1^+ channel) [10–12], and this drawback persists in despite various improvements provided by its extensions [13–18], including higher-order QRPA approaches [19–21]. The outcome of these attempts was that the calculations became more stable against g_{pp} variation, but at present there are still large differences among the values of the NMEs calculated with different QRPA-based methods, which do not yet provide a reliable determination of the two-neutrino double-β ($2\nu\beta\beta$) decay half-life. Therefore, although the QRPA methods do not seem to be suited to predict $2\nu\beta\beta$ decay half-lives, one can use the measured $2\nu\beta\beta$ decay half-lives to calibrate the g_{pp} parameters, which are further used to calculate the $0\nu\beta\beta$ decay NMEs [22]. Another method that recently provided NMEs for most $0\nu\beta\beta$ decay cases of interest is the Interacting Boson Model (IBM) [23]. Given the novelty of these calculations, it remains to further validate their reliability by comparison with experimental data.

Recent progress in computer power and numerical algorithms and improved nucleon-nucleon effective interactions have made possible large scale shell model calculations of $2\nu\beta\beta$ and $0\nu\beta\beta$ decay NMEs [24–26]. The main advantage of large-scale shell model calculations is that they seem to be less dependent on the effective interaction used, as far as these interactions are consistent with the general spectroscopy of the nuclei involved in the decay. Their main drawback is the limitation imposed by the exploding shell model dimensions on the size of the valence space that can be used. The most important success of large-scale shell model calculations has been the correct prediction of the $2\nu\beta\beta$ decay half-life for ^{48}Ca [24,27]. In addition, these calculations did not have to adjust any additional parameters, that is, given the effective interaction and the Gamow-Teller quenching factor extracted from the overall spectroscopy in the mass region (including β decay probabilities and charge-exchange form factors), one can reliably predict the $2\nu\beta\beta$ decay half-life of ^{48}Ca.

Clearly, there is a need to check and refine these calculations further, and to provide more details on the analysis of NMEs that can be validated by experiments. We have recently revisited [28] the $2\nu\beta\beta$ decay of ^{48}Ca using two recently proposed effective interactions for this mass region, GXPF1 and GXPF1A, and we explicitly analyzed the dependence of the double-Gamow-Teller sum entering the NME on the excitation energy of the 1^+ states in the intermediate nucleus ^{48}Sc. This sum was recently investigated experimentally [29], and it was shown that, indeed, the incoherent sum (using only absolute values of the Gamow-Teller matrix elements) would provide an incorrect NME, validating our prediction. We have also corrected by several orders of magnitude the probability of transition of the ground state (g.s.) of ^{48}Ca to the first excited 2^+ state of ^{48}Ti. Future experiments on double-β decay of ^{48}Ca (CANDLES [30] and CARVEL [31]) may reach the required sensitivity of measuring such transitions, and our results could be useful for planning these experiments.

In the present paper we continue our investigations of the double-β decay of ^{48}Ca, analyzing the $0\nu\beta\beta$ decay NME. ^{48}Ca

*horoi@phy.cmich.edu; URL:http://www.phy.cmich.edu/people/horoi

has the largest $Q_{\beta\beta}$ value, 4.271 MeV (the next largest is that of ^{150}Nd decay, 3.367 MeV), which could contribute to an increased decay probability. In addition, the high-energy γ and β radiation emitted in this process could help eliminate most of the background noise. However, the small natural abundance of this isotope, 0.187%, increases the difficulty of an experimental investigation, although new, improved separation techniques were recently proposed [32]. In addition, previous calculations [26,33] suggest that its NME is smaller, by a factor of 4–5, than those of other $\beta\beta$ emitters, such as ^{76}Ge and ^{82}Se [34]. Since these calculations were reported, it was shown that the short-range correlations (SRCs) might not have such a dramatic effect on the NME [35,36] as previously thought, and it was also shown that higher-order terms in the nucleon currents could be important [36]. In the present paper we take into account all these new developments in the analysis of the NME for $0\nu\beta\beta$ decay of ^{48}Ca, and we study the dependence of NME on the SRC parameters, on the finite-size (FS) parameter, on the average energy of the intermediate states, and on the effective interaction used for many-body calculations.

II. THE NEUTRINOLESS DOUBLE-β DECAY MATRIX ELEMENT

The $0\nu\beta\beta$ decay $(Z, A) \to (Z+2, A) + 2e^-$ requires the neutrino to be a Majorana fermion, that is, it is identical to the antineutrino. Considering only contributions from the light Majorana neutrinos [6], the $0\nu\beta\beta$ decay half-life is given by

$$\left(T^{0\nu}_{1/2}\right)^{-1} = G^{0\nu}_1 |M^{0\nu}|^2 \left(\frac{\langle m_{\beta\beta}\rangle}{m_e}\right)^2. \tag{1}$$

Here, $G^{0\nu}_1$ is the phase-space factor, which depends on the $0\nu\beta\beta$ decay energy, $Q_{\beta\beta}$, and the nuclear radius. The effective neutrino mass $\langle m_{\beta\beta}\rangle$ is related to the neutrino mass eigenstates m_k via the lepton mixing matrix U_{ek}:

$$\langle m_{\beta\beta}\rangle = \left|\sum_k m_k U^2_{ek}\right|. \tag{2}$$

The NME, $M^{0\nu}$, is given by

$$M^{0\nu} = M^{0\nu}_{\rm GT} - \left(\frac{g_V}{g_A}\right)^2 M^{0\nu}_F - M^{0\nu}_T, \tag{3}$$

where $M^{0\nu}_{\rm GT}$, $M^{0\nu}_F$, and $M^{0\nu}_T$ are the Gamow-Teller (GT), Fermi (F), and tensor (T) matrix elements, respectively. These matrix elements are defined as follows:

$$M^{0\nu}_\alpha = \sum_{m,n} \langle 0^+_f | \tau_{-m}\tau_{-n} O^\alpha_{mn} | 0^+_i\rangle, \tag{4}$$

where O^α_{mn} are $0\nu\beta\beta$ transition operators, $\alpha = ({\rm GT},\ F,\ T)$, $|0^+_i\rangle$ is the g.s. of the parent nucleus (in our case ^{48}Ca), and $|0^+_f\rangle$ is the g.s. of the granddaughter nucleus (in our case ^{48}Ti).

Given the two-body nature of the transition operator, the matrix element can be reduced to a sum of products of two-body transition densities (TBTDs) and antisymmetrized two-body matrix elements,

$$M^{0\nu}_\alpha = \sum_{j_p j_{p'} j_n j_{n'} J_\pi} {\rm TBTD}(j_p j_{p'}, j_n j_{n'}; J_\pi) \times \langle j_p j_{p'}; J^\pi T | \tau_{-1}\tau_{-2} O^\alpha_{12} | j_n j_{n'}; J^\pi T\rangle_a, \tag{5}$$

where O^α_{12} are given by

$$\begin{aligned} O^{\rm GT}_{12} &= \vec\sigma_1\cdot\vec\sigma_2 H_{\rm GT}(r),\\ O^F_{12} &= H_F(r),\\ O^T_{12} &= [3(\vec\sigma_1\cdot\hat r)(\vec\sigma_2\cdot\hat r) - \vec\sigma_1\cdot\vec\sigma_2] H_T(r). \end{aligned} \tag{6}$$

The matrix elements of O^α_{12} for the jj coupling scheme consistent with the conventions used by modern shell model effective interactions are described in the Appendix.

To calculate the two-body matrix elements in Eq. (5) one needs the neutrino potentials entering into the radial matrix element $\langle nl|H_\alpha|nl'\rangle$ in Eq. (A1). Following Ref. [36] and using closure approximation, one gets

$$H_\alpha(r) = \frac{2R}{\pi}\int_0^\infty f_\alpha(qr)\frac{h_\alpha(q^2)}{q+\langle E\rangle} G_\alpha(q^2) q dq, \tag{7}$$

where $f_{F,{\rm GT}}(qr) = j_0(qr)$ and $f_T(qr) = j_2(qr)$ are spherical Bessel functions, $\langle E\rangle$ is the average energy of the virtual intermediate states used in the closure approximation, and the form factors $h_\alpha(q^2)$ that include the higher-order terms in the nucleon currents are

$$\begin{aligned} h_F(q^2) &= g^2_V(q^2),\\ h_{\rm GT}(q^2) &= \frac{g^2_A(q^2)}{g^2_A}\left[1 - \frac{2}{3}\frac{q^2}{q^2+m^2_\pi} + \frac{1}{3}\left(\frac{q^2}{q^2+m^2_\pi}\right)^2\right] + \frac{2}{3}\frac{g^2_M(q^2)}{g^2_A}\frac{q^2}{4m^2_p},\\ h_T(q^2) &= \frac{g^2_A(q^2)}{g^2_A}\left[\frac{2}{3}\frac{q^2}{q^2+m^2_\pi} - \frac{1}{3}\left(\frac{q^2}{q^2+m^2_\pi}\right)^2\right] + \frac{1}{3}\frac{g^2_M(q^2)}{g^2_A}\frac{q^2}{4m^2_p}. \end{aligned} \tag{8}$$

The $g_{V,A,M}$ form factors in Eq. (8) can include nucleon FS effects, which, in the dipole approximation, are given by

$$\begin{aligned} g_V(q^2) &= \frac{g_V}{\left(1+q^2/\Lambda^2_V\right)^2},\\ g_M(q^2) &= (\mu_p - \mu_n) g_V(q^2),\\ g_A(q^2) &= \frac{g_A}{\left(1+q^2/\Lambda^2_A\right)^2}. \end{aligned} \tag{9}$$

Here $g_V = 1$, $g_A = 1.25$, $(\mu_p - \mu_n) = 3.7$, $\Lambda_V = 850$ MeV, and $\Lambda_A = 1086$ MeV.

The SRCs are included via the correlation function $f(r)$ that modifies the relative wave functions at short distances,

$$\psi_{nl}(r) \to [1 + f(r)]\psi_{nl}(r), \tag{10}$$

where $f(r)$ can be parametrized as [36]

$$f(r) = -ce^{-ar^2}(1 - br^2). \tag{11}$$

Recently, the UCOM method of including SRCs [37] was used for analyzing $0\nu\beta\beta$ decay matrix elements [36,38]. Reference [36] indicates that the UCOM SRC eliminates the effects of the FS, and in addition, it slightly violates some general properties of the Fermi and Gamow-Teller matrix elements (see, e.g., Ref. [36], p. 3). We decided not to include the UCOM SRCs in our analysis. The radial matrix elements of H_α between relative harmonic oscillator wave functions $\psi_{nl}(r)$ and $\psi_{n'l'}(r)$, $\langle nl|H_\alpha(r)|n'l'\rangle$, become

$$\int_0^\infty r^2 dr \psi_{nl}(r) H_\alpha(r) \psi_{n'l'}(r)[1 + f(r)]^2. \tag{12}$$

Although the neutrino potentials are quite close to a Coulomb potential, the integrands in Eq. (7) are strongly oscillating, and the integrals require special numerical treatment. Having calculated the two-body matrix elements, we developed a shell model approach for computing the many-body matrix elements for $0\nu\beta\beta$ transition, Eq. (5). This approach is briefly described in the Appendix.

Reference [39] reports a QRPA decomposition of the NME of ^{100}Mo on the spin and parity of the intermediate states, and contemplating the large contribution of the negative-parity states in this case, it suggests that the shell model calculations would underestimate the NME because of the limited valence spaces they can use. In particular, in our case we limit ourselves to the pf model space in which one cannot construct any negative-parity state in the intermediate nucleus, ^{48}Sc. We can show, however, that under the reasonable assumption that ^{40}Ca is a good core, and considering only $0\hbar\omega$ correlations in the g.s. wave functions of ^{48}Ca and ^{48}Ti, the contribution of the negative states in the intermediate nucleus is zero. For example, assuming that nucleons from the sd shell can be excited in the odd-odd nucleus ^{48}Sc, using the isospin symmetry, the closure condition, and the two-body nature of the $0\nu\beta\beta$ transition operators O^α, one could get an additional contribution to the pf part of the NME of the form

$$\langle 0_f^+ T = 2|O^\alpha(1\hbar\omega)|0_f^+ T = 4\rangle, \tag{13}$$

where

$$O^\alpha(1\hbar\omega) = \sum \tilde{O}^\alpha_{fdfd}[(a_f^\dagger \tilde{a}_f)^{t_f}(a_d^\dagger \tilde{a}_d)^{t_d}]^{\Delta T}. \tag{14}$$

Here the index f labels pf states, and the index d labels sd states. Because the sd core is completely filled up in both the initial and the final wave function, the sd particle-hole product in Eq. (14) can only couple to $t_d = 0$, and therefore in Eq. (14) $\Delta T = t_f \leqslant 1$. One can conclude that this additional contribution is zero, because it cannot account for the $\Delta T = 2$ transition between the initial and the final state. Under our assumptions, similar contributions from other major shells are also zero. Including weak $2\hbar\omega$ contributions in the initial and the final g.s. wave functions would result in small contributions from the negative-parity states in the intermediate nucleus, but these contributions would require a renormalization of the pf part of the effective interaction, and a direct comparison with the present results would be rather difficult. We plan to investigate these effects further and report the results in a forthcoming publication.

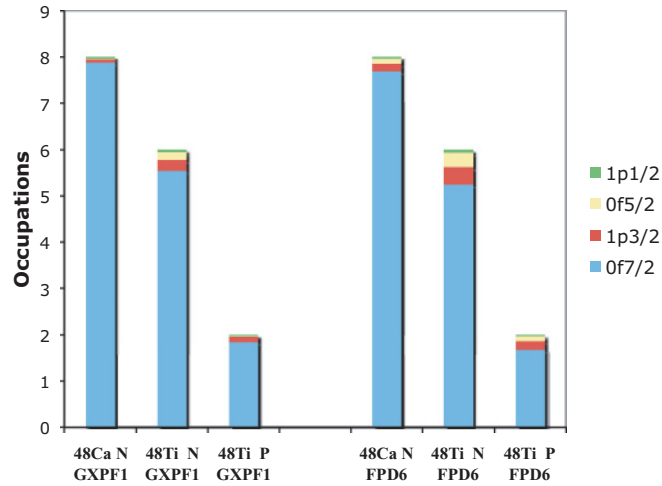

FIG. 1. (Color online) Comparison of neutron and proton occupation probabilities between the GXPF1 interaction and the FPD6 interaction.

III. RESULTS

In this study of the $0\nu\beta\beta$ decay NME we used five different effective interactions available for the shell model description of the pf-shell nuclei: GXPF1 [40], GXPF1A [41], KB3 [42], KB3G [43], and FPD6 [44]. These effective interactions were constructed starting from a G matrix [45] in the pf shell, which was further adjusted to describe some specific (but different) sets of experimental energy levels of some pf-shell nuclei. Although their matrix elements are quite different, their predictions of the spectroscopic observables around $A = 48$ are not very far apart. Recent experimental investigations [46,47] of the nucleon occupation probabilities in ^{76}Ge and ^{76}Se and the subsequent theoretical analysis

TABLE I. Neutron and proton occupation probabilities for nuclei involved in the decay.

Nucleus (N/P)	Interaction	$0f_{7/2}$	$1p_{3/2}$	$0f_{5/2}$	$1p_{1/2}$
^{48}Ca N	GXPF1	7.883	0.073	0.033	0.011
^{48}Ti N	GXPF1	5.545	0.237	0.167	0.051
^{48}Ti P	GXPF1	1.846	0.110	0.033	0.011
^{48}Ca N	GXPF1A	7.892	0.067	0.032	0.009
^{48}Ti N	GXPF1A	5.535	0.248	0.168	0.048
^{48}Ti P	GXPF1A	1.839	0.119	0.032	0.010
^{48}Ca N	KB3	7.800	0.0706	0.105	0.024
^{48}Ti N	KB3	5.422	0.266	0.248	0.064
^{48}Ti P	KB3	1.770	0.120	0.089	0.022
^{48}Ca N	KB3G	7.795	0.070	0.112	0.024
^{48}Ti N	KB3G	5.416	0.260	0.263	0.061
^{48}Ti P	KB3G	1.763	0.120	0.097	0.021
^{48}Ca N	FPD6	7.693	0.161	0.117	0.029
^{48}Ti N	FPD6	5.253	0.369	0.310	0.068
^{48}Ti P	FPD6	1.673	0.196	0.101	0.031

TABLE II. Parameters for the short-range correlation (SRC) parametrization of Eq. (11).

SRC	a	b	c
Miller-Spencer	1.10	0.68	1.00
CD-Bonn	1.52	1.88	0.46
AV18	1.59	1.45	0.92

TABLE III. Different contributions to the NME for the GXPF1A interaction with $\langle E \rangle = 7.72$ MeV.

SRC	$M^{0\nu}_{\rm GT}$	$M^{0\nu}_{F}$	$M^{0\nu}_{T}$	$M^{0\nu}$
None	0.556	−0.219	−0.015	0.711
Miller-Spencer	0.465	−0.141	−0.014	0.570
CD-Bonn	0.688	−0.222	−0.014	0.845
AV18	0.634	−0.204	−0.014	0.779

[36,48] highlighted the relevance of these observables for obtaining an accurate description of the nuclear structure of the nuclei involved in double-β decay. Figure 1 compares the neutron and proton occupation probabilities in ^{48}Ca and ^{48}Ti for two different effective interactions, GXPF1 and FPD6. One can see very small differences between the results of the two interactions. One can come to the same conclusion when comparing similar occupation probabilities for all five interactions reported in Table I.

In the present calculations we considered both SRC effects and FS effects. Although the radial dependence of the neutrino potential is very close to that of a Coulomb potential, many previous calculations [25,26,33,34] took into account the SRC missing in the two-body-product wave functions, via the Jastrow-like parametrization described in Eqs. (10)–(12). Until recently, the parameters a, b, and c used were those proposed by Miller and Spencer [49], which have the effect of decreasing the NME by about 30%. Recently, [36] the SRC effects were revisited, using modern nucleon-nucleon interactions, such as CD-Bonn and AV18, and it was found that the decrease in the relative wave functions at short distances is compensated by a relative increase at longer distances, and the overall NMEs do not change very much compared with the NMEs without SRC effects. Reference [36] proposed a parametrization of these results in terms of similar Jastrow-like correlation functions as in Eqs. (10) and (11); the corresponding parameters are listed in Table II. In addition, Ref. [35] introduced an effective $0\nu\beta\beta$ operator that takes into account the SRC effects and the contribution of the missing shells from the valence space using the general theory of effective interactions [45] and found that the NME for the $0\nu\beta\beta$ decay of ^{82}Se did not change significantly compared with the result of the "bare" operator.

Figure 2 shows our NMEs for all five effective interactions, for all three SRC sets of parameters listed in Table II, and for no SRC. One can see that the preceding semiquantitative analysis is reflected in the dependence of the NME on the choice of SRC. The results do not show significant dependence on the effective interaction used, although one can see a 20% spread of NMEs for the same choice of SRC. All NMEs reported here contain the higher-order terms described in Eqs. (7)–(9). A comparison with the NMEs calculated without the higher-order terms in the potential will be reported elsewhere. To be consistent [50] with the calculation of the phase factor $G^{0\nu}_1$, we used $R = 1.2A^{1/3}$ fm in Eq. (7). Our choice for the $\hbar\omega$ parameter entering the harmonic oscillator wave functions was $45A^{-1/3} - 25A^{-2/3}$, which was shown to provide a better shell model description of observables than the simple $41A^{-1/3}$ ansatz. Table III lists the GT, F, and T contributions to the overall NMEs for all SRC choices, when the GXPF1A interaction was used. One can see that all these contributions add coherently in Eq. (3) and that the tensor contribution is negligible in all cases.

Figure 3 shows the dependence of the NMEs of the average energy of the intermediate states. Varying $\langle E \rangle$ from 2.5 to 12.5 MeV, one gets less than 5% variation in the NME. This

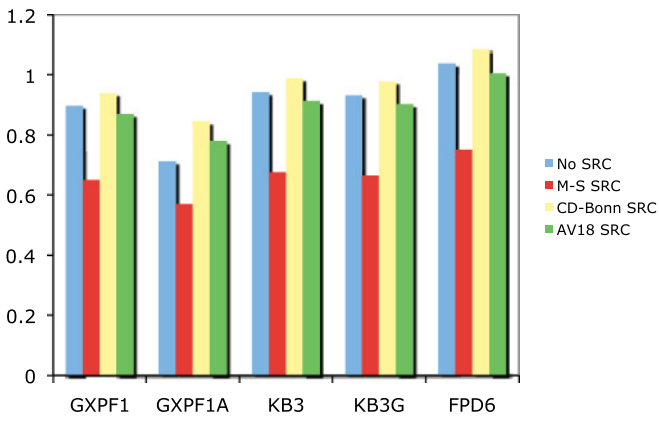

FIG. 2. (Color online) Dependence of the NME on the effective interaction used and the short-range correlation (SRC) model. M-S, Miller-Spencer.

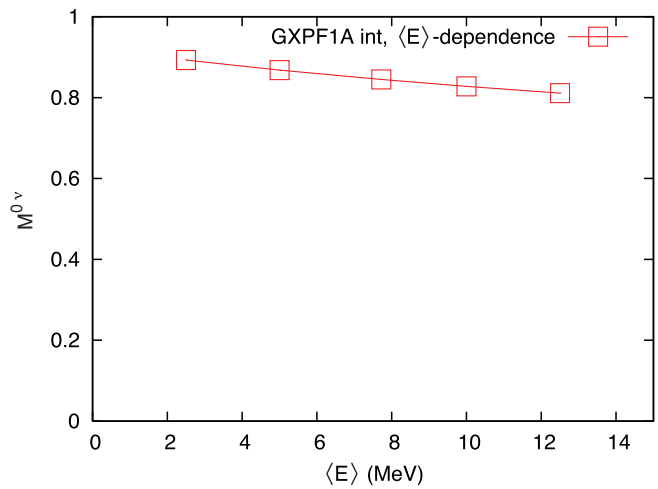

FIG. 3. (Color online) Dependence of the NME on the average energy of the intermediate states $\langle E \rangle$ for the GXPF1A interaction.

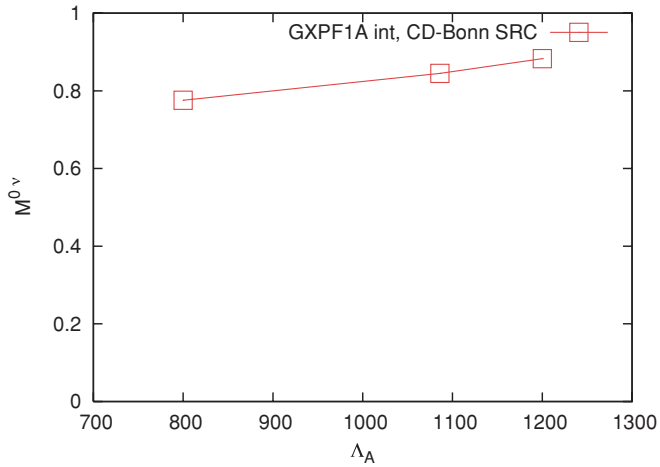

FIG. 4. (Color online) Dependence of the NME on the axial cutoff parameter Λ_A for the GXPF1A interaction.

result suggests that the closure approximation is quite good, although a direct study might be necessary to determine the exact magnitude of the error. All other NME results reported here used $\langle E \rangle = 7.72$ MeV. Figure 4 shows the dependence of the NME of the axial cutoff parameter Λ_A, with Λ_V kept fixed at 850 MeV. The variation is within 5%, indicating a weak dependence of the FS cutoff parameters. The FS effects were implemented via the cutoff parameters Λ_V and Λ_A in the form factors given in Eq. (9). In most of our results, except those in Fig. 4, we use the same FS cutoff parameters as in Refs. [6] and [36], that is, $\Lambda_V = 850$ MeV and $\Lambda_A = 1086$ MeV. In Fig. 4 we present the dependence of the NME on Λ_A, with Λ_V kept at its nominal value. As with the $\langle E \rangle$ dependence, the results vary by less than 5%.

Similar, but less complete, results on the $0\nu\beta\beta$ decay of ^{48}Ca were recently reported in Refs. [33] and [38], and Ref. [38] reports the ^{48}Ca NMEs including the higher-order terms in the nucleon currents, but only for the KB3 interaction and without the new SRC models of Ref. [36]. Reference [33] reports results for three effective interactions, but without including the higher-order terms in the nucleon currents or the new SRC models of Ref. [36]. For cases where we use similar models, our results seem to be consistent with those of Refs. [33] and [38].

IV. CONCLUSIONS AND OUTLOOK

In conclusion, we have presented a new shell model analysis of the NMEs for neutrinoless double-β decay of ^{48}Ca. We included in the calculations the recently proposed higher-order terms of nucleon currents, three old and recent parametrizations of the SRC effects, FS effects, and effects of changing the average energy of the intermediate states. We also treated carefully the few other parameters entering into the calculations. We found very small variation in the NMEs with the average energy of the intermediate states or FS cutoff parameters and moderate variation versus the effective interaction and SRC parametrization. We have also shown that if the g.s. wave functions of the initial and final nucleus can be accurately described using only pf orbitals, the contribution from the negative-parity states of the intermediate nucleus ^{48}Sc can be neglected.

Our overall average NME using all values presented in Fig. 2 is 0.86, although elimination of the Miller-Spencer SRC parametrization would significantly increase this value. We estimate the error owing to the effects studied here to be about 18%. Using the present value of the NME and the recommended [50] phase-space factor $G_1^{0\nu} = 6.5 \times 10^{-14}$ yr^{-1}, one can conclude that a future measurement of the $0\nu\beta\beta$ decay half-life of 10^{26} yr, which seems to be the limit imposed by the present energy resolution of the CANDLES detector [32] (see also Fig. 21 in Ref. [51]), could detect a neutrino mass $\langle m_{\beta\beta} \rangle$ of about 230 ± 45 meV. New improvements in detector technology could further reduce this limit.

We believe that our analysis has covered the most important effects relevant to the accuracy of the NME for the double-β decay of ^{48}Ca. The successful prediction of the $2\nu\beta\beta$ decay half-live of ^{48}Ca using the shell model approach in the same model space suggests that the $0\nu\beta\beta$ decay half-life could be reliably predicted. Our analysis indicates that closure approximation is accurate at the level of 5% error. However, a direct comparison with the sum on intermediate states, calculated within the shell model, would be more reassuring.

As in all other $0\nu\beta\beta$ decay calculations reported so far, no quenching factors have been used. This is probably the least investigated potential effect on the $0\nu\beta\beta$ decay NME. It is possible that the GT-like operators are quenched even if they have finite range. No definitive conclusion exists about these effects, although Ref. [35] seems to indicate that they might not play a major role. One could try gaining some insight into this problem by investigating the fictitious $0\nu\beta\beta$ decay of a light nucleus, such as ^{16}Be, and by increasing the valence space one could study the changes in different contributions to the NME.

ACKNOWLEDGMENTS

M.H. acknowledges support from NSF Grant No. PHY-0758099. S.S. acknowledges the support from the ANCS Project PN09370106.

APPENDIX

The matrix element of O_{12}^{α} for nonantisymmetrized jj-coupling two-particle states can be decomposed into products of reduced matrix elements of the spin, relative, and center of mass operators,

$$\begin{aligned}\langle n_1 l_1 j_1, n_2 l_2 j_2; J^\pi T = 1 | O_{12}^{\alpha} | n_1' l_1' j_1', n_2' l_2' j_2'; J^\pi T = 1 \rangle \\ = \sum_{S\lambda} \left\langle l_1 \frac{1}{2}(j_1), l_2 \frac{1}{2}(j_2) \middle| \frac{1}{2}\frac{1}{2}(S), l_1 l_2(\lambda) \right\rangle_J \\ \times \left\langle l_1' \frac{1}{2}(j_1'), l_2' \frac{1}{2}(j_2') \middle| \frac{1}{2}\frac{1}{2}(S), l_1' l_2'(\lambda) \right\rangle_J \\ \times \frac{1}{\sqrt{(2S+1)}} \left\langle \frac{1}{2}\frac{1}{2}; S \| S_\alpha^{(0)} \| \frac{1}{2}\frac{1}{2}; S \right\rangle\end{aligned}$$

$$\times \sum_{nn'lNL} \langle nl, NL|n_1 l_1, n_2 l_2\rangle_\lambda \times \langle n'l, NL|n'_1 l'_1, n'_2 l'_2\rangle_\lambda \langle nl|H_\alpha(r)|n'l\rangle, \tag{A1}$$

where

$$\left\langle l_1 \frac{1}{2}(j_1), l_2 \frac{1}{2}(j_2) \middle| \frac{1}{2}\frac{1}{2}(S), l_1 l_2(\lambda) \right\rangle_J = \sqrt{(2j_1+1)(2j_2+1)(2S+1)(2\lambda+1)} \begin{pmatrix} l_1 & \frac{1}{2} & j_1 \\ l_2 & \frac{1}{2} & j_2 \\ \lambda & S & J \end{pmatrix} \tag{A2}$$

and the last factor is a $9j$ symbol. As mentioned in the text, the order of the spin-orbit coupling must be consistent with the convention considered in the derivation of the effective interaction used for the many-body calculations ($\vec{l}+\vec{s}$ in most cases). The reduced spin matrix elements are

$$\left\langle \frac{1}{2}\frac{1}{2}S \| \vec{\sigma}_1 \cdot \vec{\sigma}_2 \| \frac{1}{2}\frac{1}{2}S \right\rangle = \sqrt{2S+1}\,[2S(S+1)-3], \qquad \left\langle \frac{1}{2}\frac{1}{2}S \| 1 \| \frac{1}{2}\frac{1}{2}S \right\rangle = \sqrt{2S+1}. \tag{A3}$$

The expressions for the matrix elements of the tensor operator will be given elsewhere. Our calculations show that the tensor term makes a small contribution to the NME in most cases. The higher-order terms in the nucleon currents, however, decrease the overall NME by about 20%–25%. The antisymmetrized form of the two-body matrix elements can be obtained using

$$\langle j_p j_{p'}; J^\pi T|t_{-1}t_{-2}O^\alpha_{12}|j_n j_{n'}; J^\pi T\rangle_a = \frac{1}{\sqrt{(1+\delta_{j_p j'_{p'}})(1+\delta_{j_n j_{n'}})}} \times [\langle j_p j_{p'}; J^\pi T|t_{-1}t_{-2}O^\alpha_{12}|j_n j_{n'}; J^\pi T\rangle - (-1)^{j_n+j_{n'}+J}\langle j_p j_{p'}; J^\pi T|t_{-1}t_{-2}O^\alpha_{12}|j_{n'} j_n; J^\pi T\rangle]. \tag{A4}$$

Having the two-body matrix elements ready, one can calculate the NME in Eq. (5) if TBTD($j_p j_{p'}, j_n j_{n'}; J_\pi$) values are known. Most of the shell model codes do not provide TBTDs. One alternative approach is to take advantage of the isospin symmetry that most of the effective interactions have, which creates wave functions with good isospin. The approach described here also works when the proton and neutron are in different shells. If these conditions are satisfied, one can transform the two-body matrix elements of a $\Delta T = 2$ operator using the Wigner-Eckart theorem, from $\Delta T_z = -2$ to $\Delta T_z = 0$, which can be further used (see below) to describe transitions between states of the same nucleus. Denoting

$$\left\langle O^{\Delta T=2}_{\Delta T_z=-2} \right\rangle = \langle T=1\ T_z=-1|O^{\Delta T=2}_{\Delta T_z=-2}|T=1\ T_z=1\rangle, \tag{A5}$$

one gets for $\Delta T_z = 0$ the two-body matrix elements

$$\langle pp|O^{\Delta T=2}_{\Delta T_z=0}|pp\rangle = \langle nn|O^{\Delta T=2}_{\Delta T_z=0}|nn\rangle = \left\langle O^{\Delta T=2}_{\Delta T_z=-2} \right\rangle \times C^{1\ 2\ 1}_{1\ 0\ 1} \Big/ C^{1\ \ 2\ \ 1}_{1\ -2\ -1}, \tag{A6}$$

and

$$\langle pn\ T=1|O^{\Delta T=2}_{\Delta T_z=0}|pn\ T=1\rangle = \left\langle O^{\Delta T=2}_{\Delta T_z=-2} \right\rangle \times\ C^{1\ 2\ 1}_{0\ 0\ 0} \Big/ C^{1\ \ 2\ \ 1}_{1\ -2\ -1}, \tag{A7}$$

where $C^{1\ \ 2\ \ 1}_{T_{zi}\ \Delta T_z\ T_{sf}}$ are isospin Clebsch-Gordan coefficients. The transformed matrix elements in Eqs. (A6) and (A7) preserve spherical symmetry and they can be used as a piece of a Hamiltonian, $H^\alpha_{\beta\beta}$, that violates isospin symmetry.

One can then lower by 2 units the isospin projection of the g.s. of the parent nucleus that has the higher isospin $T_>$, ^{48}Ca in our case, thus becoming an isobar analog state of the granddaughter nucleus that has isospin $T_< = T_> - 2$, ^{48}Ti in our case. Denoting by $|0^+_{i<}\ T_>\rangle$ the transformed state, one can now calculate the many body-matrix elements of the transformed $0\nu\beta\beta$ operator,

$$M^{0\nu}_\alpha(T_z = T_<) = \langle 0^+_f\ T_<|H^\alpha_{\beta\beta}|0^+_{i<}\ T_>\rangle. \tag{A8}$$

Choosing $|0^+_{i<}\ T_>\rangle$ as a starting Lanczos vector and performing one Lanczos iteration with $H^\alpha_{\beta\beta}$, one gets

$$H^\alpha_{\beta\beta}|0^+_{i<}\ T_>\rangle = a_1|0^+_{i<}\ T_>\rangle + b_1|L\rangle, \tag{A9}$$

where $|L_1\rangle$ is the new Lanczos vector. Then one can calculate the matrix elements in Eq. (A8):

$$M^{0\nu}_\alpha(T_z = T_<) = b_1\langle 0^+_f\ T_<|L_1\rangle. \tag{A10}$$

The transition matrix elements in Eq. (5) can then be recovered using, again, the Wigner-Eckart theorem,

$$M^{0\nu}_\alpha = M^{0\nu}_\alpha(T_z = T_<) \times C^{T_>\ 2\ T_<}_{T_>\ -2\ T_<} \Big/ C^{T_>\ 2\ T_<}_{T_<\ 0\ T_<}. \tag{A11}$$

Although it looks complicated, this procedure is rather easy to implement. The transformation of the g.s. of the parent to an analog state of the granddaughter can be performed very quickly, and one Lanczos iteration represents a small load compared with the calculation of the g.s. of the granddaughter. The additional calculations described in Eqs. (A8)–(A10) require smaller resources than those necessary to calculate the TBTDs. This procedure has the advantage that it can be implemented using public shell model codes, such as Antoine [52].

[1] W. C. Haxton and G. J. Stephenson, Prog. Part. Nucl. Phys. **12**, 409 (1984).

[2] J. Suhonen and O. Civitarese, Phys. Rep. **300**, 123 (1998).

[3] A. Faessler and F. Simkovic, J. Phys. G **24**, 2139 (1998).

[4] H. V. Klapdor-Kleingrothaus, *60 Years of Double-Beta Decay—From Nuclear Physics to Beyond Standard Model Particle Physics* (World Scientific, Singapore, 2001).

[5] S. R. Elliot and P. Vogel, Annu. Rev. Nucl. Part. Sci. **52**, 115 (2002).

[6] F. T. Avignone, S. R. Elliot, and J. Engel, Rev. Mod. Phys. **80**, 481 (2008).
[7] B. Aharmim *et al.*, Phys. Rev. C **72**, 055502 (2005).
[8] C. Arsepella *et al.*, Phys. Lett. **B658**, 101 (2008); T. Araki *et al.*, Phys. Rev. Lett. **94**, 081801 (2005).
[9] T. Schwetz, Nucl. Phys. B (Proc. Suppl) **188**, 158 (2008).
[10] P. Vogel and M. R. Zirnbauer, Phys. Rev. Lett. **57**, 3148 (1986).
[11] K. Grotz and H. V. Klapdor, Nucl. Phys. **A460**, 395 (1986).
[12] J. Suhonen, T. Taigel, and A. Faessler, Nucl. Phys. **A486**, 91 (1988).
[13] A. Staudt, K. Muto, and H. V. Klapdor-Kleingrothaus, Europhys. Lett. **13**, 31 (1990).
[14] O. Civitarese, A. Faessler, J. Suhonen, and X. R. Wu, Phys. Lett. **B251**, 333 (1990).
[15] S. Stoica and W. A. Kaminski, Phys. Rev. C **47**, 867 (1993); S. Stoica, *ibid.* **49**, 2240 (1994); Phys. Lett. **B350**, 152 (1995); S. Stoica and I. Mihut, Nucl. Phys. **A602**, 197 (1996); S. Stoica and H. V. Klapdor-Kleingrothaus, *ibid.* **A694**, 269 (2001).
[16] A. A. Raduta, D. S. Delion, and A. Faessler, Phys. Rev. C **51**, 3008 (1995).
[17] G. Pantis, F. Simkovic, J. D. Vergados, and A. Faessler, Phys. Rev. C **53**, 695 (1996).
[18] A. Bobyk, W. A. Kaminski, and P. Zareba, Eur. Phys. J. A **5**, 385 (1999); Nucl. Phys. **A669**, 221 (2000).
[19] A. A. Raduta, A. Faessler, S. Stoica, and W. A. Kaminski, Phys. Lett. **B254**, 7 (1991); A. A. Raduta, A. Faessler, and S. Stoica, Nucl. Phys. **A534**, 149 (1991).
[20] J. Toivanen and J. Suhonen, Phys. Rev. Lett. **75**, 410 (1995); Phys. Rev. C **55**, 2314 (1997).
[21] F. Simkovic, J. Schwieger, M. Veselsky, G. Pantis, and A. Faessler, Phys. Lett. **B393**, 267 (1997).
[22] V. A. Rodin, A. Faessler, F. Šimkovic, and P. Vogel, Nucl. Phys. **A766**, 107 (2006); **A793**, 213(E) (2007).
[23] J. Barea and F. Iachello, Phys. Rev. C **79**, 044301 (2009).
[24] E. Caurier, A. Poves, and A. P. Zuker, Phys. Lett. **B252**, 13 (1990).
[25] E. Caurier, F. Nowacki, A. Poves, and J. Retamosa, Phys. Rev. Lett. **77**, 1954 (1996).
[26] J. Retamosa, E. Caurier, and F. Nowacki, Phys. Rev. C **51**, 371 (1995).
[27] A. Balysh, A. De Silva, V. I. Lebedev, K. Lou, M. K. Moe, M. A. Nelson, A. Piepke, A. Pronskiy, M. A. Vient, and P. Vogel, Phys. Rev. Lett. **77**, 5186 (1996).
[28] M. Horoi, S. Stoica, and B. A. Brown, Phys. Rev. C **75**, 034303 (2007).
[29] K. Yako *et al.*, Phys. Rev. Lett. **103**, 012503 (2009).
[30] S. Umehara *et al.*, J. Phys. Conf. Ser. **39**, 356 (2006).
[31] Yu. G. Zdesenko *et al.*, Astropart. Phys. **23**, 249 (2005).
[32] I. Ogawa, Bull. Am. Phys. Soc. **54**(10), 19 (2009).
[33] A. Poves, E. Caurier, and F. Nowacki, Eur. Phys. J. A **36**, 195 (2008); arXiv:0709.0277 (2007).
[34] E. Caurier, J. Menendez, F. Nowacki, and A. Poves, Phys. Rev. Lett. **100**, 052503 (2008).
[35] J. Engel and G. Hagen, Phys. Rev. C **79**, 064317 (2009).
[36] F. Simkovic, A. Faessler, H. Muther, V. Rodin, and M. Stauf, Phys. Rev. C **79**, 055501 (2009).
[37] R. Roth, H. Hergert, P. Papakonstantinou, T. Neff, and H. Feldmeier, Phys. Rev. C **72**, 034002 (2005).
[38] J. Menendez, A. Poves, E. Caurier, and F. Nowacki, Nucl. Phys. **A818**, 139 (2009).
[39] F. Simkovic, A. Faessler, V. Rodin, P. Vogel, and J. Engel, Phys. Rev. C **77**, 045503 (2008).
[40] M. Honma, T. Otsuka, B. A. Brown, and T. Mizusaki, Phys. Rev. C **69**, 034335 (2004).
[41] M. Honma, T. Otsuka, B. A. Brown, and T. Mizusaki, Eur. Phys. J. A **25** (Suppl. 1), 499 (2005).
[42] A. Poves and A. P. Zuker, Phys. Rep. **71**, 141 (1981).
[43] A. Poves *et al.*, Nucl. Phys. **A694**, 157 (2001).
[44] W. A. Richter, M. G. van der Merwe, R. E. Julies, and B. A. Brown, Nucl. Phys. **A523**, 325 (1991).
[45] M. Hjorth-Jensen, T. T. S. Kuo, and E. Osnes, Phys. Rep. **261**, 125 (1995).
[46] J. Schiffer *et al.*, Phys. Rev. Lett. **100**, 112501 (2008).
[47] B. P. Kay *et al.*, Phys. Rev. C **79**, 021301(R) (2009).
[48] J. Menendez, A. Poves, E. Caurier, and F. Nowacki, Phys. Rev. C **80**, 048501 (2009).
[49] G. A. Miller and J. E. Spencer, Ann. Phys. (NY) **100**, 562 (1976).
[50] S. Cowell, Phys. Rev. C **73**, 028501 (2006).
[51] F. T. Avignone III, G. S. King III, and Yu. G. Zdesenko, New J. Phys. **7**, 6 (2005).
[52] E. Caurier and F. Nowacki, Acta Phys. Pol. **30**, 705 (1999); http://sbgat194.in2p3.fr/∼theory/antoine/menu.html.